# INFRARED RADIATIVE PROPERTIES OF YTTRIA-STABILIZED ZIRCONIA THERMAL BARRIER COATINGS

J.I. Eldridge, C.M. Spuckler, and K.W. Street
NASA Glenn Research Center
Cleveland, OH 44135

J.R. Markham
Advanced Fuel Research, Inc.
East Hartford, CT 06108

## ABSTRACT

The infrared (IR) transmittance and reflectance of translucent thermal barrier coatings (TBCs) have important implications for both the performance of these coatings as radiation barriers and emitters as well as affecting measurements of TBC thermal conductivity, especially as TBCs are being pushed to higher temperatures. In this paper, the infrared spectral directional-hemispherical transmittance and reflectance of plasma-sprayed 8wt% yttria-stabilized zirconia (8YSZ) TBCs are reported. These measurements are compared to those for single crystal YSZ specimens to show the effects of the plasma-sprayed coating microstructure. It is shown that the coatings exhibit negligible absorption at wavelengths up to about 5 μm, and that internal scattering rather than surface reflections dominates the hemispherical reflectance. The translucent nature of the 8YSZ TBCs results in the absorptance/emittance and reflectance of TBC-coated substrates depending on the TBC thickness, microstructure, as well as the radiative properties of the underlying substrate. The effects of these properties on TBC measurements and performance are discussed.

## INTRODUCTION

The infrared (IR) radiative properties of thermal barrier coatings (TBCs) are an important concern because the most widely used TBCs are composed of yttria-stabilized zirconia (YSZ), which is translucent over a wavelength region where thermal radiation tends to be concentrated. It has been recognized by previous researchers that, because of this translucency, the absorption and emission of thermal radiation by TBC-coated substrates is produced not just by the TBC surface, but by the entire coating/substrate system.[1-6] This translucency raises several issues for the high temperature perfomance of TBCs and for the measurement of any properties dependent on surface temperature. Specifically, pyrometer temperature measurements penetrate into the coating and will not provide real surface temperature measurements, thereby leading to overestimates of thermal conductivity. Furthermore, radiant heating used to produce a thermal gradient or thermal pulse will not be entirely absorbed at the TBC surface, introducing additional errors in thermal conductivity or diffusivity measurements. More importantly, TBC translucency may undermine its performance at high temperatures since YSZ-based TBCs have been designed to minimize heat conduction, but not to provide a barrier to thermal radiation. For example, a translucent TBC does not provide a barrier to external radiation, which can then be absorbed directly by the substrate. In addition,

thermal radiation generated within the coating will result in the hotter outer sections of the TBC heating the inner cooler sections, thereby decreasing the $\Delta T$ across the TBC. As we move towards higher temperature application of TBCs, these radiative contributions to TBC performance will increase in relative importance.

Recent efforts have been made to better understand the temperature dependence of the radiative properties of both electron-beam physical vapor deposited[7] and plasma-sprayed[8] YSZ-based TBCs. However, these studies have either concentrated on TBC-coated specimens systems or on radiative property measurements at specific wavelengths. The objective of the present study was to perform systematic characterization of the radiative properties of freestanding plasma-sprayed 8 wt% yttria-stabilized zirconia (8YSZ), examining the effects of coating thickness, temperature, sintering, and substrate contribution. The emphasis was placed on freestanding 8YSZ TBCs in order to better understand the radiative behavior of the coatings without the complicating substrate effects that can be difficult to separate. Comparisons were also made to radiative properties of single crystal YSZ to elucidate the effects of the plasma-sprayed coating microstructure. Finally, the implications of the radiative properties of 8YSZ TBCs on TBC property measurement and on TBC performance were assessed.

## EXPERIMENT

The 8YSZ TBC specimens were prepared by plasma-spraying 8YSZ powder with an average particle size of about 60 μm onto sacrificial carbon disks (1 in. diameter x 0.125 in. thick) using a plasma-spray coating system equipped with a 6-axis industrial robot. Heating the TBC-coated carbon disks in air for 2 hr at 800°C burned off the carbon substrates and produced freestanding 8YSZ coatings. Both sides of the freestanding coatings were lightly polished to a 15 μm finish to remove large surface asperities that would prevent meaningful thickness measurements. A micrometer was used to measure the coating thickness. Fig. 1 illustrates the microcracked, porous, and lamellar nature of the coating's plasma-spray microstructure.

Because the TBCs were highly scattering, hemispherical detection was necessary to fully capture the reflected or transmitted IR radiation. Room-temperature spectral directional-hemispherical reflectance and transmittance spectra were obtained for the TBC specimens using a Nicolet Magna 760 FTIR spectrometer equipped with a Labsphere RSA-NI-550ID integrating sphere accessory. Spectra in the 0.8-2.5 μm wavelength range were collected using a quartz halogen lamp source and a $CaF_2$ beamsplitter. Spectra in the 2-25 μm wavelength range were collected using an Ever-Glo Mid-IR source and a KBr beamsplitter. All spectra were acquired using an uncooled deuterated triglycidyl sulfate (DTGS) detector.

High-temperature hemispherical-directional reflectance and transmittance spectra were obtained at Advanced Fuel Research, using their benchtop emissometer. Unlike the room temperature directional-hemispherical measurements, where the incident radiation is collimated and the reflected or transmitted radiation is collected over a full hemisphere, the high-temperature hemispherical-directional measurements use a reciprocal arrangement where the TBC is illuminated diffusely and hemispherically and then the reflected or transmitted radiation is detected in only one direction (near normal). A hemi-ellipsoidal mirror is used to focus the radiation from a near-blackbody source uniformly onto the TBC, which is heated to the desired temperature with a torch; the near-normal reflected or transmitted radiation is reflected into an interferometer where the FTIR spectrum is obtained; a baseline specimen thermal radiation spectrum is subtracted to obtain the true reflectance or tranmsittance spectrum. A detailed description of the high-temperature spectrometer has been reported.[9] Spectra in the 0.8-1.2 μm wavelength range were collected with an uncooled Si detector, and spectra in the 1.2-20 μm range were collected with a liquid nitrogen cooled mercury cadmium telluride (MCT) detector.

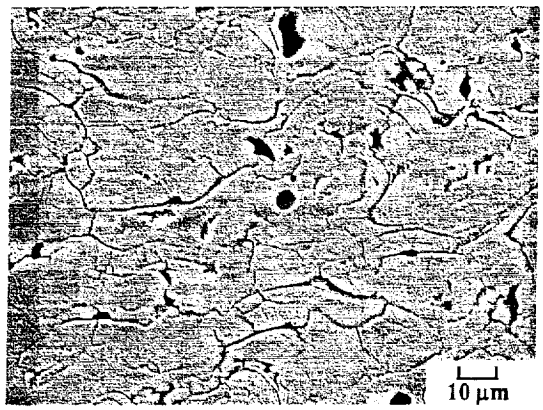


**Figure 1. SEM micrograph of polished cross section of plasma-sprayed 8YSZ TBC. Plasma-spray direction is from top to bottom.**

Under the conditions of uniform irradiation provided by the benchtop emissometer, the hemispherical-directional measurements are equivalent to the directional-hemispherical measurements collected in the room temperature spectrometer.[10] Because of this equivalence, all measurements will be referred to simply as hemispherical reflectance or transmittance measurements.

RESULTS

***(100) Single Crystal 13.5YSZ***

In order to determine the radiative properties intrinsic to YSZ so that these could later be separated from the effects of the TBC microstructure, room temperature hemispherical transmittance and reflectance spectra (Fig. 2a-b) were collected from (100) single crystal 13.5YSZ one-inch diameter disks (MTI Corp.) ranging in thickness from 0.28 to 1.01 mm. It was believed that the compositional difference between the 13.5YSZ single crystals and the 8YSZ plasma-sprayed coatings would not produce large differences in radiative behavior. Hemispherical emittance/absorptance spectra (Fig. 2c) were obtained by closure and Kirchoff's law using the relationship E = A = 1-R-T, where E is hemispherical emittance, A is hemispherical absorptance, R is hemispherical reflectance, and T is hemispherical transmittance. Fig. 2a shows that the single crystal radiative behavior can be divided into three radiative regions. In region I (< 5 μm), the single crystals are perfectly transparent (confirmed by zero absorption in Fig. 2c) and the transmittance has no thickness dependence; losses are only due to reflections from the front and back surfaces (Fig. 2b). In region III (> 10 μm), the single crystals are completely opaque (zero transmittance) with high absorptance (Fig. 2c). Of special note, is the existence of a wavelength around 12.5 μm where the coating shows near-blackbody behavior (E ≈1 in Fig 2c). Region II is the transition region, where due to partial absorption, the transmittance exhibits a thickness dependence. This transmittance thickness dependence is well modeled by simple zero-scattering exponential absorption:

$$T = \frac{(1-\rho)^2 e^{-\mu_a x}}{1-\rho^2 e^{-2\mu_a x}} \approx (1-\rho)^2 e^{-\mu_a x} \qquad (1)$$

where $\rho$ is the surface reflectance, $\mu_a$ is the absorption coefficient, and x is the specimen thickness. Fig. 3 shows $\mu_a$ determined by applying Equation 1 to the ratio of the transmittance of the 0.47 mm thick specimen to the transmittance of the 0.28 mm thick specimen.

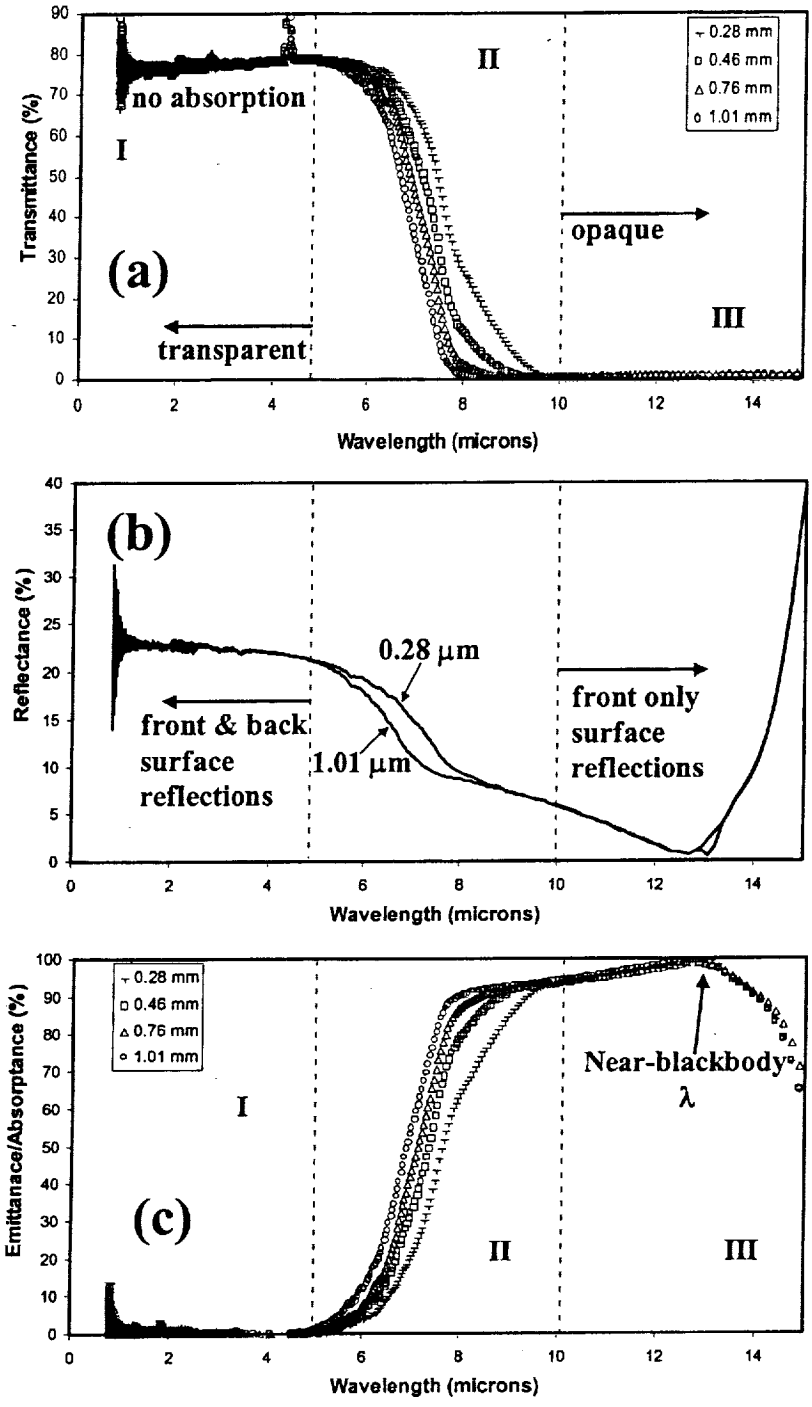


Figure 2. Room-temperature hemispherical transmittance (a), reflectance (b), and emittance/absorptance (c) of (100) single crystal 13.5YSZ specimens of various thicknesses.

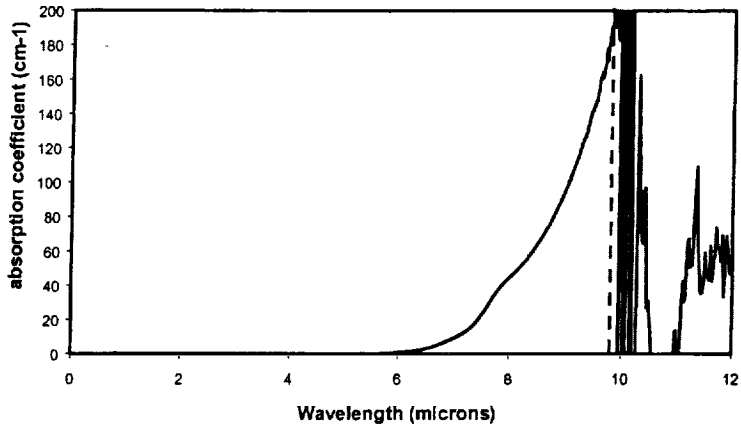


**Figure 3. Absorption coefficient as function of wavelength determined by transmittance ratio method for (100) single crystal 13.5YSZ.**

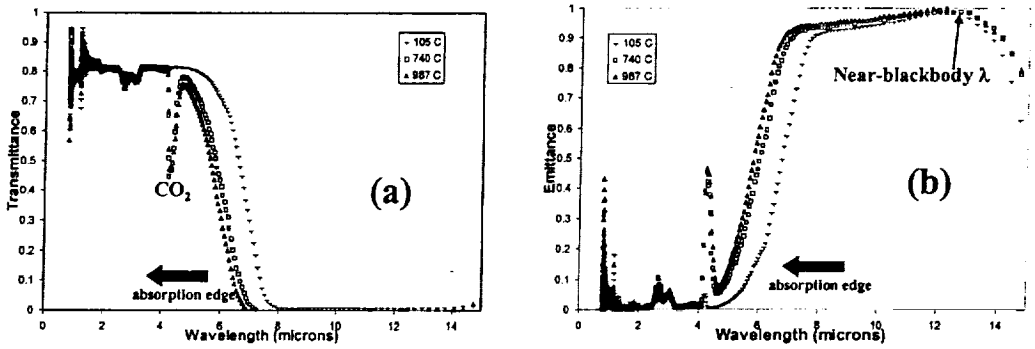


**Figure 4. Room-temperature hemispherical transmittance (a), reflectance (b), and emittance/absorptance (c) of freestanding plasma-sprayed 8YSZ coatings of various thicknesses.**

High-temperature hemispherical transmittance and emittance/absorptance spectra of the 1-mm-thick 13.5YSZ single crystal (Fig. 4) show the same three-region behavior as the room temperature spectra, except the absorption edge (transition from transparency to opacity in region II) moves to shorter wavelengths as the temperature increases. The peak or dip just above 4 μm is an artifact due to $CO_2$ ambient absorption. It should be noted that the near-blackbody wavelength near 12.5 μm is maintained at all temperatures.

***Plasma-Sprayed 8YSZ***

Room-temperature hemispherical transmittance, reflectance, and emittance/absorptance spectra are shown in Fig. 5 for freestanding plasma-sprayed 8YSZ coatings ranging in thickness from 125 to 680 μm. One significant difference with the single crystal spectra is the appearance of a large absorption peak near 3 μm wavelength that can be ascribed to OH bound within the plasma-sprayed 8YSZ structure. More importantly, the transmittance and reflectance spectra (Figs. 5a,b) clearly show the highly scattering nature of the plasma-spray coatings. Unlike the thickness-

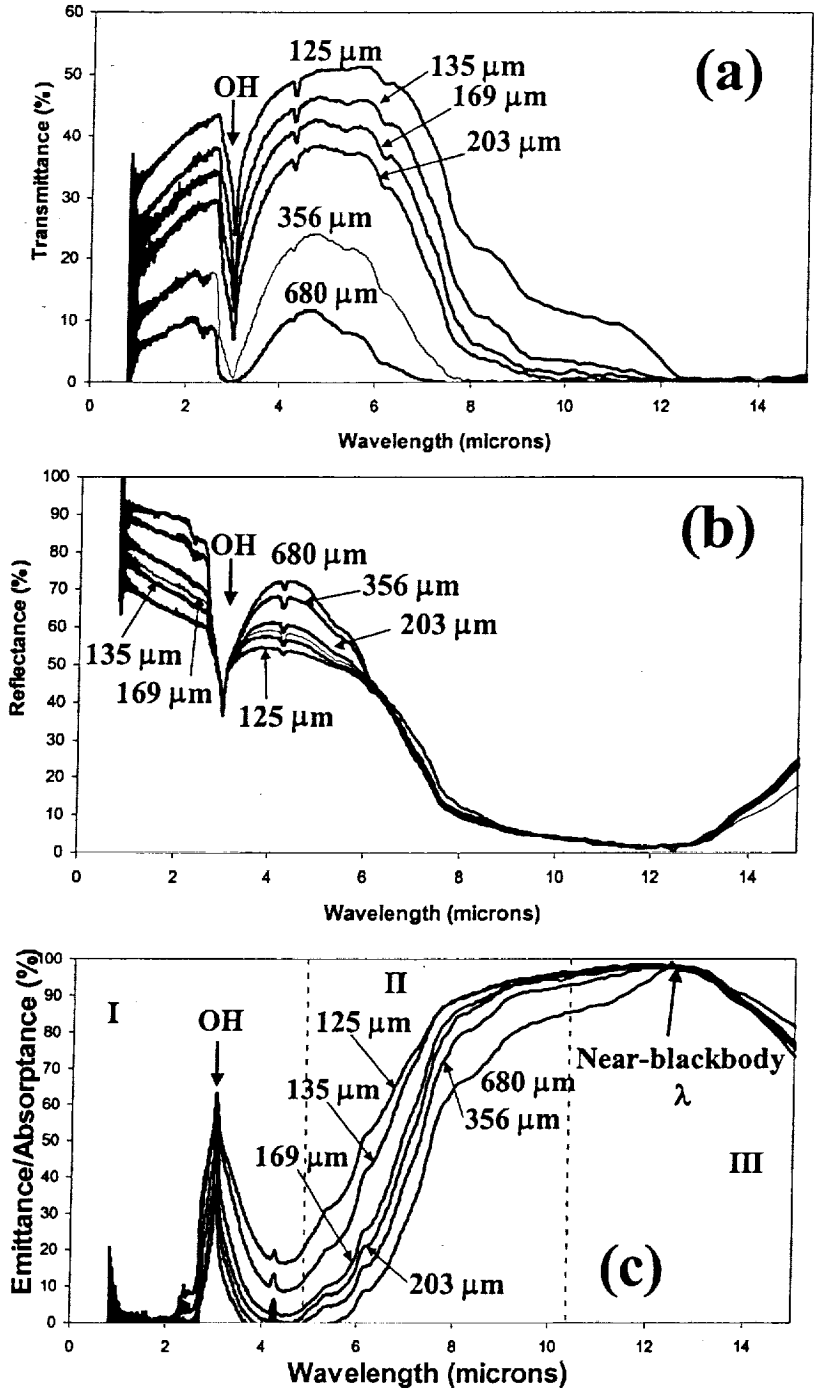


Figure 5. Room-temperature hemispherical transmittance (a), reflectance (b), and emittance/absorptance (c) of freestanding plasma-sprayed 8YSZ coatings of various thicknesses

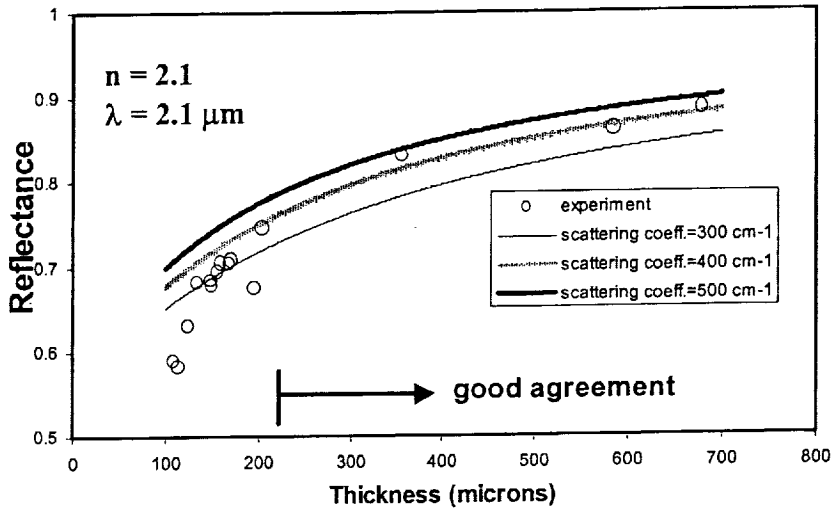


**Figure 6. Measured room-temperature hemispherical reflectances vs. specimen thickness (open circles) for freestanding plasma-sprayed 8YSZ coatings. Continuous lines represent reflectances calculated for selected scattering coefficients using Equation 2.**

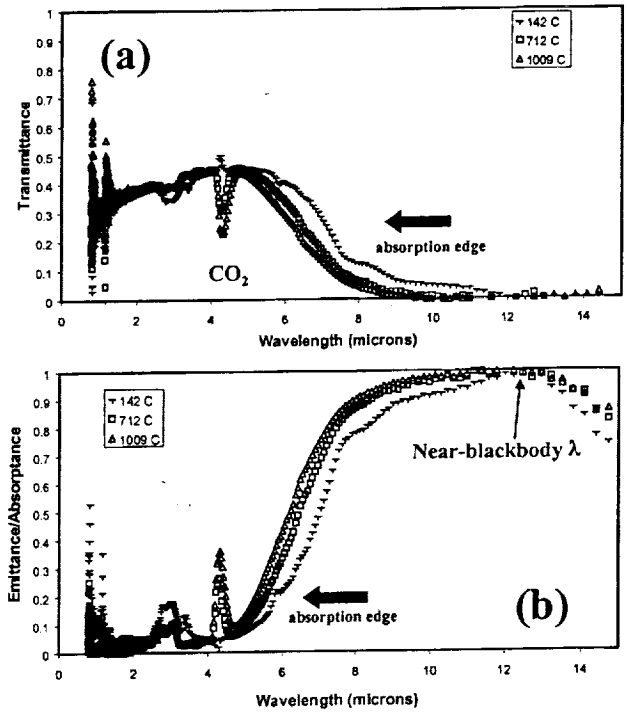


**Figure 7. Temperature dependence of hemispherical transmittance (a) and emittance/absorptance (b) for 112 μm thick freestanding plasma-sprayed 8YSZ.**

independent transmittances and reflectance observed for the single crystal specimens (Fig. 2a,b) in region I (< 5 μm wavelength), the plasma-sprayed coatings show a decrease in transmittance with increasing coating thickness. However, this decrease in transmittance (Fig. 5a) with coating thickness is counterbalanced by an equal increase in coating reflectance (Fig. 5b), such that, like the single crystal YSZ, there is zero emittance/absorptance below 5 μm wavelength, except in the region of OH absorption (Fig. 5c). The transmission losses in region I are due to a combination of surface reflections and volume scattering; a fraction of the scattered radiation is increased coating thickness and becomes greater with shorter wavelengths. For thick specimens and short wavelengths, reflectances greater than 90% were achieved (compared to maximum reflectance below 25% for single crystals – see Fig. 2b). The hemispherical transmittance and reflectance in region I was modeled by a zero-absorption Kubelka-Munk model which estimates the transmittance through a purely scattering material by the relationship:

$$T = \frac{n^2}{\frac{1+\rho}{1-\rho} + \mu_s x} \qquad (2)$$

where n is the index of refraction, ρ is the internal interface reflectance, $\mu_s$ is the scattering coefficient, and the layer reflectance was determined by closure (R=1-T). Fig. 6 displays reflectance data measured at a wavelength of 2.1 μm (in region I) along with curves calculated from Equation 2 for n=2.1 and for scattering coefficients of 300, 400, and 500 $cm^{-1}$. The data show good agreement with a scattering coefficient of 400 $cm^{-1}$. Measurements of specimens thinner than 200 μm may be below the calculated curve because the two-flux Kubelka-Munk model assumes that scattering causes the incident collimated radiation becomes perfectly diffuse immediately upon entering the specimen. In reality, the transition to diffuse radiation occurs over a finite specimen thickness.

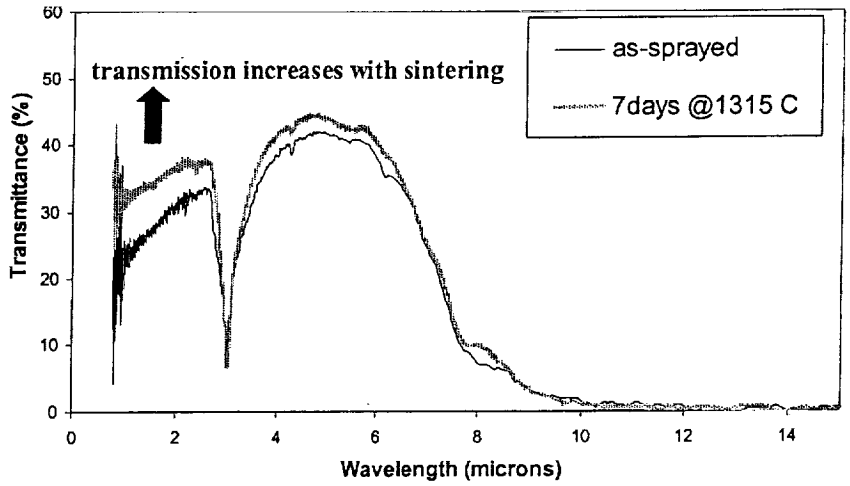


**Figure 8. Room-temperature hemispherical transmittance of 160 μm thick freestanding plasma-sprayed 8YSZ before and after heat-treatment for 7 days at 1315°C in air.**

High-temperature hemispherical transmittance and emittance/absorptance spectra of the 112-μm thick plasma-sprayed 8YSZ coating (Fig. 7) show the same behavior as the room temperature spectra (Fig. 5), except that the absorption edge (transition from translucency to opacity in region II) moves to shorter wavelengths as the temperature increases. An important observation is that the emittance/absorptance in the translucent region I remains near zero even up to 1000°C. Also, similar to the single crystal specimens, the plasma-sprayed 8YSZ specimens show near-blackbody behavior (E≈1) at a wavelength near 12.5 μm for all thicknesses and temperatures measured.

The effect of sintering on coating radiative properties was evaluated by collecting hemispherical transmittance and reflectance measurements for a 160 μm thick freestanding plasma-sprayed 8YSZ specimen before and after heat treatment for seven days at 1315°C in air. Fig. 8 shows that the hemispherical transmittance increases significantly (particularly for shorter wavelengths) after the heat treatment; reflectance measurements showed a counterbalancing decrease in reflectance for shorter wavelengths that can be interpreted as a decrease in volume scattering after heat treatment.

Finally, the effect of coating substrate was evaluated by comparing hemispherical emittance/absorptance for a freestanding coating with that for coatings with a carbon or superalloy (Rene 5) plus bond coat (NiCrAlY) substrate (Fig. 9). The significantly higher emittances at wavelengths less than 8 μm for coatings on a substrate indicate that the bulk of the emittance/absorptance observed for the TBC-coated substrates originates from the substrate itself, with higher system emittances being measured for higher emittance substrates (carbon).

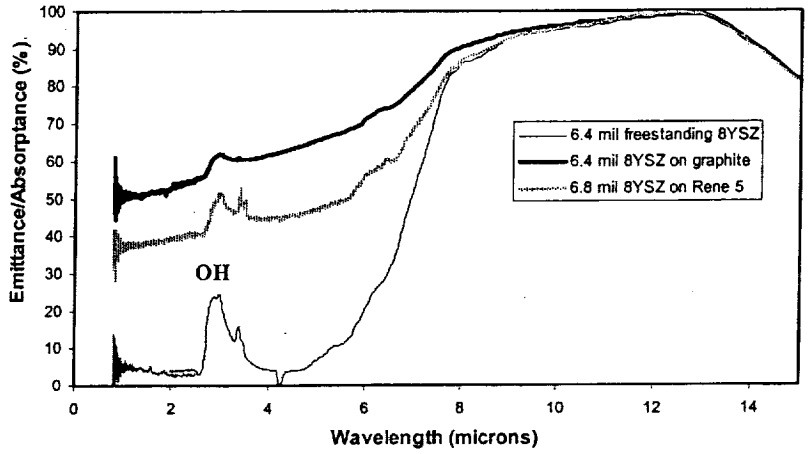


**Figure 9. Comparison of room-temperature hemispherical emittance of plasma-sprayed 8YSZ coatings without substrate and with either carbon or superalloy substrate.**

DISCUSSION

The IR radiative behavior of plasma-sprayed 8YSZ TBCs can be divided into three wavelength regions. In region I (< 5 μm), the coatings exhibit nearly complete translucency (Fig. 5c); neglibile absorption is observed except that associated with OH absorption. In contrast to the transparent single crystal 13.5YSZ specimens, the hemispherical reflectance and transmittance (Fig. 5a,b) show an increase in reflectance along with a complimentary decrease in transmittance with increasing specimen thickness due to volume scattering that is well described by the zero-

absorption Kubelka-Munk two-flux model for thicknesses greater than 200 μm. The high degree of scattering is likely associated with the high density of scattering defects (microcracks and pores) in the plasma-spray microstructure. (Fig. 1) In region III (> 10 μm), the coatings are nearly opaque due to high absorption. Region II (5 to 10 μm) is where increasing absorption produces a transition between translucency (region I) and opacity (region III). It should be noted that while absorption increases with increasing wavelength, the scattering decreases. The primary effect of increasing the specimen temperature is to move region II (the absorption edge) to shorter wavelengths (Fig. 7), with no emittance/absorption produced in region I. This lack of emittance/absorptance at short IR wavelengths should not be extrapolated beyond the highest temperatures measured here (1000°C), as several reports indicate that YSZ loses its translucency at temperatures above 1200°C.[11-12] We plan to perform tests at higher temperatures to confirm this change in radiative behavior in TBCs. The IR radiative behavior discussed above has several implications for TBC temperature measurements and TBC performance as discussed below.

***TBC Temperature Measurement***

Because of the usual requirement of non-invasive, non-contact temperature measurements, TBC surface temperatures are usually measured with IR pyrometers. For many materials, pyrometers operating in the 1-3 μm wavelength region are used for temperature measurements around 1000°C to take advantage of the maximum in the blackbody thermal radiation intensity (Fig. 10) as well as maximum temperature-intensity sensitivity observed in this wavelength region. However, YSZ has near-zero emittance in this region and therefore near-zero thermal radiation intensity, even at 1000 °C. (Fig. 10)

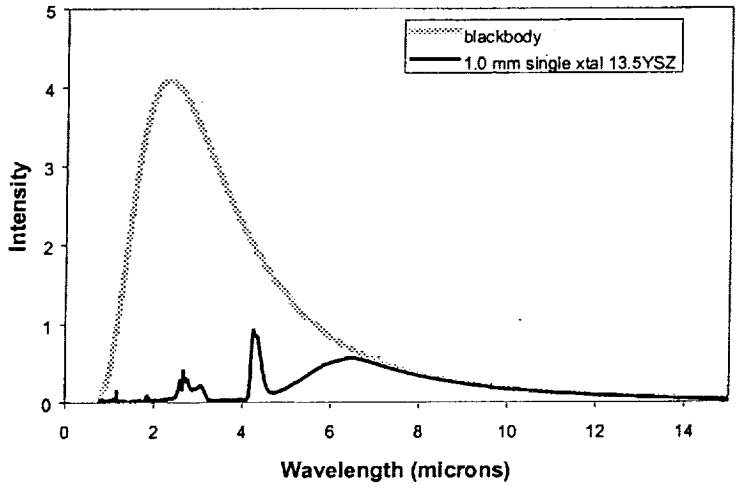


**Figure 10. Comparison of radiation intensity at 1000°C from blackbody and from 1.0 mm thick (100) single crystal 13.5YSZ.**

Applying an opaque environmentally stable "black" layer to the surface of the TBC can circumvent the TBC translucency. This approach provides a true surface temperature and can take advantage of the peak blackbody thermal radiation intensity. However, the opaque layer will change the heat transfer mechanisms due to a change in boundary conditions. The opaque layer

will absorb radiation that would have been reflected and transmitted by the TBC, and will raise the TBC surface temperature. While the surface temperature will be accurate, it may not be the surface temperature obtained by the TBC without an opaque coating. In addition, the opaque layer will thermally radiate at wavelengths at which the TBC is translucent, producing direct radiative substrate heating that would be absent without the opaque layer; at high temperatures this radiative heat source at the substrate surface will lower $\Delta T$ across the coating and therefore increase the apparent thermal conductivity obtained from the relationship $q = -k\Delta T/x$, where q is the heat flux, k is the thermal conductivity, and x is the coating thickness.

An alternative approach is to take advantage of the near-blackbody wavelength at 12.5 μm, where the coating is naturally opaque. Unlike the case of an applied opaque surface layer, the heat transfer mechanisms will be those intrinsic to the TBC, and the hot TBC surface cannot radiate at wavelengths where the underlying TBC is transparent. Because of the high absorption at 12.5 μm, pyrometer measurements using this wavelength will provide true surface temperatures. Also, with $E \approx 1$ ($R \approx 0$), the detected radiant energy will not contain any significant reflected contributions from the hot environment; this condition is essential for successful temperature measurements in hot environments such as in engine tests. In addition, the near-blackbody wavelength at 12.5 μm is the only wavelength where the YSZ-based TBC is insensitive to coating thickness, temperature, sintering (ageing), or addition of other rare-earth dopants. This emittance insensitivity is extremely attractive since the pyrometer temperature measurement is determined from the relationship:

$$R_{specimen}(\lambda,T) = \varepsilon_{specimen}(\lambda,T,thickness,etc.)R_{BB}(\lambda,T) \quad (3)$$

where $R_{specimen}(\lambda,T)$ is the radiant intensity from the specimen at wavelength $\lambda$ and temperature T, $\varepsilon_{specimen}$ is the specimen emittance, and $R_{BB}(\lambda,T)$ is the radiant intensity from a blackbody at wavelength $\lambda$ and temperature T. The near-blackbody wavelength therefore offers the tremendous advantage of not requiring a determination of $\varepsilon_{specimen}$ for every change in coating thickness, temperature, or other variable. The disadvantage of this approach is the lower radiation intensity and temperature sensitivity; however, researchers have shown that fast long-wavelength temperature measurements can be achieved with temperature accuracies within several °C.[13]

***TBC Performance***

The translucent character of plasma-sprayed 8YSZ TBCs will significantly affect TBC performance at high temperatures; however, the optimum TBC radiative properties for thermal protection of the substrate depend on the thermal environment and must be evaluated on a case-by-case basis. For example, for the extreme case of pure radiative heating, maximum TBC reflectance is desired to reject the incident radiation. On the other extreme, with pure convective heating with cool surrounding walls (e.g., burner rig testing), maximum TBC emittance (minimum reflectance) is desired for thermal radiative cooling. The following discussion will focus only on how the TBC radiative properties affect the contribution of radiative heating of the TBC and substrate.

Because the plasma-sprayed 8YSZ TBCs provide no IR absorption (except for OH absorption) at least up to 1000°C in wavelength region I (< 5 μm), where the greatest intensity of external blackbody radiation will be concentrated at high temperatures (Fig. 10), any IR radiation that is not reflected will be absorbed by the substrate, increasing the substrate temperature due to direct radiative heating and will therefore reduce $\Delta T$ through the TBC. Therefore, when rejection of external radiation is the primary goal, the TBC reflectance in region I should be maximized.

While internally generated thermal radiation is not a factor in wavelength region I where the TBC has zero emittance/absorptance (therefore no radiative heat transfer within TBC), internally generated radiation will be important in region II where both IR emission and reabsorption occur over distances much larger than atomic dimensions. Because the hotter outer layers of the TBC radiate more energy than the cooler inner layers, this thermal emission and reabsorption process will reduce $\Delta T$, effectively increasing the TBC thermal conductivity. Increasing radiative scattering in this wavelength region (depending on the absorption) will decrease the radiative mean-free-path (distance covered between emission and reabsorption) to the point where the radiative heat transfer can be treated as a radiative diffusion problem where $qr=-k_r\Delta T$, where $k_r=16\sigma T^3/(3a_R)$ and $a_R$ is the Rosseland mean absorption coefficient.[10] If the absorption coefficient is high enough (as in region III), the radiation component disappears.

Fortunately, the plasma-sprayed 8YSZ TBCs are highly scattering, especially at shorter wavelengths, producing much higher hemispherical reflectances than single crystal YSZ (Figs. 2b, 5b). The effect of volume scattering in wavelength region I (< 5 μm) can be used to advantage to reflect incident external radiation and avoid direct radiative heating of the substrate. Fig. 6 shows that increasing the optical thickness of the TBC can increase the hemispherical reflectance. This can be accomplished by either increasing the actual thickness or by increasing the scattering coefficient. The scattering coefficient can be increased by engineering increased porosity or microcracks with dimensions on the order of the IR wavelengths of interest. Note, however, that diminishing returns are gained by further increases in optical thickness. Another factor that greatly affects the coating/substrate reflectance is the reflectance of the substrate (effect of substrate on emittance shown in Fig. 9). Using a more specific version of Equation 2 that allows different reflectances at the top and bottom interfaces of the TBC, Fig. 11 shows the effect of substrate reflectance on TBC/substrate coating reflectance. Note that the effect of substrate reflectance is greatest for smaller optical thicknesses and that quite high substrate reflectances (> 80%) are required to better the reflectance of a freestanding coating, which has approximately 80% total internal reflection due to the index of refraction difference.

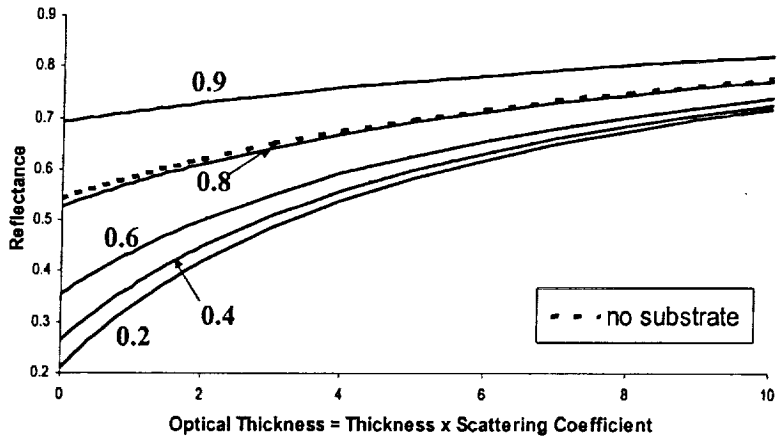


**Figure 11. Calculated hemispherical reflectance for a non-absorbing, scattering TBC deposited onto substrates with various reflectances.**

## CONCLUSIONS

Hemispherical transmittance and reflectance measurements showed that plasma-sprayed 8YSZ TBCs retain a translucent (near zero absorption) region below 5 μm wavelength up to 1000°C, although the transition between the translucent to opaque wavelength regions moves to shorter wavelengths with increased temperature. In contrast to the nonscattering 13.5YSZ single crystals, the plasma-sprayed coatings exhibited substantial effects of volume scattering that produced thickness-dependent transmittance/reflectance in the translucent wavelength region that was well described by a zero-absorption Kubelka-Munk two-flux model except for the thinnest coatings.

Pyrometer temperature measurements at the near-blackbody wavelength of about 12.5 μm are highly recommended to provide true surface measurements, to eliminate error-producing reflections originating from a hot environment, and for emittance insensitivity to TBC thickness, temperature, sintering, and other variables that all would require emittance corrections using other wavelengths. Opaque surface coatings can also achieve these benefits. However, opaque surface coatings also change the heat transfer boundary conditions, thereby changing the surface temperature and introducing a component of direct radiative substrate heating that would otherwise be absent.

Finally, although YSZ provides no intrinsic barrier to radiation at wavelengths shorter than 5 μm, highly reflecting TBCs can be produced through a combination of volume scattering by an engineered microstructure and by inserting a highly reflective layer between the TBC and the substrate.

## ACKNOWLEDGMENTS

The authors wish to thank R.A. Miller, D. Zhu, and D.L. Ng for helpful discussions, G.L. Leissler for plasma-spraying, and Q. Nguyen for assistance with SEM.

## REFERENCES

1. C.H. Liebert, "Emittance and Absorptance of the National Aeronautics and Space Administration Ceramic Thermal Barrier Coating," Thin Solid Films, **53**, 235-240 (1978).
2. S. Wahiduzzaman and T. Morel, "Effect of Translucence of Engineering Ceramics on Heat Transfer in Diesel Engines," Oak Ridge National Laboratory Report ORNL/Sub/88-22042/2, Oak Ridge, TN, April 1992.
3. C.M. Spuckler and R. Siegel, "Refractive Index and Scattering Effects on Radiative Behavior of a Semitransparent Layer", J. Thermophys. Heat Transfer, 7[2], 302-310 (1993).
4. R. Siegel, "Internal Radiation Effects in Zirconia Thermal Barrier Coatings," J. Thermophys., 10[4], 707-709 (1996).
5. R. Siegel and C.M. Spuckler, "Analysis of Thermal Radiation Effects on Temperatures in Turbine Engine Thermal Barrier Coatings," Mater. Sci. Eng. A, 245, 150-159 (1998).
6. P.G. Klemens and M. Gell, "Thermal Conductivity of Thermal Barrier Coatings," Mater. Sci. Eng. A, 245, 143-149 (1998).
7. J. Manara, R. Brandt, J. Kuhn, J. Fricke, T. Krell, U. Schulz, M. Peters, W.A. Kaysser, "Emittance of $Y_2O_3$ Stabilised $ZrO_2$ Thermal Barrier Coatings Prepared by Electron-Beam Physical-Vapour Deposition," High Temp. High Pressures, 32, 361-368 (2000).
8. A. Ferriere, L. Lestrade, J.-F. Robert, "Optical Properties of Plasma-Sprayed $ZrO_2$-$Y_2O_3$ at High Temperature for Solar Applications," J. Solar Energy Eng., 122, 9-13 (2000).
9. J.R. Markham, K. Kinsella, R.M. Carangelo, C.R. Brouillette, M.D. Carangelo, P.E. Best, and P.R. Solomon, "Bench Top Fourier Transform Infrared Based Instrument for

Simultaneously Measuring Surface Spectral Emittance and Temperature," Rev. Sci. Instrum., 64[9], 2515-2522 (1993).
10. R. Siegel and J.R. Howell, "Thermal Radiation Heat Transfer," 4th ed., Taylor & Francis, NY, 2002.
11. F. Cabannes and D. Billard, "Measurement of Infrared Absorption of Some Oxides in Connection with the Radiative Transfer in Porous and Fibrous Materials," Int. J. Thermophys., 8[1], 97-118 (1987).
12. F.A. Akopov, G.E. Val'yano, A.Y. Borob'ev, V.N. Mineev, V.A. Petrov, A.P. Chernyshev, and G.P. Chernyshev, "Thermal Radiative Properties of Ceramic of Cubic ZrO2 Stabilized with Y2O3 at High Temperatures," High Temp., 39[2], 244-254 (2001).
13. H. Latvakoski, J. Markham, M. Borden, T. Hawkins, and M. Cybulsky, "Measurement of Advanced Ceramic Coated Superalloys with a Long Wavelength Pyrometer," AIAA Report 2000-2212, 21st AIAA Aerodynamic Measurement Technology and Ground Testing Conference, June 2000.